DOI: 10.15480/882.9298

Eighth International Symposium on Marine Propulsors
smp'24, Berlin, Germany, March 2024

Investigation of conventional and highly-skewed tip-raked propeller performance

Mohammed Islam, Moqin He

National Research Council of Canada (NRC-OCRE), St. John's, NL, Canada

ABSTRACT

Over the last few decades, several attempts have been made by maritime R & D to obtain higher propulsive efficiencies and lower cavitation and pressure pulses (and hence underwater radiated noise, URN) by skewing the propeller blades and radically modifying the geometry in the blade tip region. Efforts to design such high-skewed tip-raked propellers focused mainly on increasing the propeller's efficiency, with little to no attention given to minimizing the cavitation and URN. This work was initiated to develop tools for evaluating the propulsive and cavitation performance of a conventional and a highly-skewed propeller, with and without the tip-rake of different magnitudes and orientations, all designed for the same operating conditions. The authors used an existing in-house numerical codebase, PaTH-AC, capable of predicting the hydrodynamic performance of screw propellers, as a primary tool for the investigation. The radial skew distributions and the rake around the blade tip are varied systematically, and their effects are evaluated using PaTH-AC analysis for open water and cavitation performance. The evaluated variants include forward-raked and aftward-raked propellers with and without specific skew distributions.

The predictions of the open water performance of a Base propeller have been validated using both basin measurements and high-fidelity RANS simulations in the corresponding operating conditions. The RANS predicted thrust and torque of the highly-skewed Base propeller compare well with the corresponding measurements; however, the PaTH-AC results show slight over-predictions of both thrust and torque. Additionally, RANS simulations were carried out for one case of a tip-rake propeller, which was used to validate the PaTH-AC predictions. Overall, the results of the predictions show better propulsive performance of the forward-raked propellers, particularly with moderate rake change at the tip. In light loading conditions, RANS and PaTH-AC predicted similar blade tip and pressure side sheet cavitation. The PaTH-AC is currently being further developed for more accurate cavitation predictions and to predict the URN induced by the propellers using the predicted pressure field on the blade surface. The results presented here are considered preliminary.

Keywords

Tip-fin propellers, tip-rake propellers, highly-skewed propellers, open water characteristics, panel method, RANS, CFD, and cavitation performance.

1 INTRODUCTION

The propeller design significantly influences ships' powering performance and acoustics (pressure pulse-induced hull vibrations and underwater radiated noise, URN) optimization. A newly designed propeller's performance is generally characterized by its open-water hydrodynamic performance, cavitation characteristics, pressure pulse and URN behaviours. Different geometrical aspects of propeller blades often determine these propeller performance aspects. Many unconventional concepts, such as variable geometric parameter distributions, have been investigated to improve one or multiple of these often-conflicting characteristics. This research addresses one such unconventional concept which includes the radical modification of the blade tip rake propeller.

The tip-rake propeller can be divided into two categories according to the rake direction of the blade tip, namely, the propeller with the tip section(s) that bends toward the pressure side (aftward-raked propeller), e.g., the CLT (Contracted and Tip-Loaded) propeller, and the propeller with a tip rake that is inclined to the suction side (forward-raked propeller), e.g., the Kappel propeller (see Figure 1, Dang 2004). These tip bends alter propeller efficiency by shifting the spanwise circulation distribution toward the tip of the propeller blade while using geometric features to prevent losses over the blade tips (Brown et al 2014). The tip-raked propellers share

similarities with the winglet mounted onto the aerofoil, which can hinder the flow around the blade tip and thus exaggerate the pressure difference of the blade surface, i.e., the positive component of the thrust (Prandtl & Betz 1927). The aftward-raked propellers are characterized by possibly reduced tip vortex cavitation. Therefore, these propellers can afford a higher load at the tip without having an increased intensity of tip vortex cavitation. However, these propellers are more sensitive to changes in inflow and circulation than conventional propellers (Klose et al 2017). The present studies are confined to propellers with tip rakes to both the pressure and the suction sides with different slopes of the rake values.

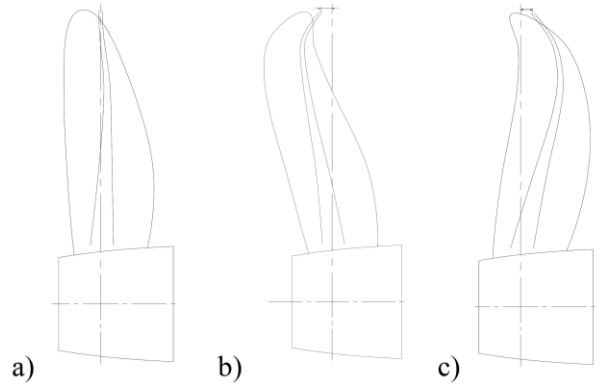

Figure 1 a) rake = 0 (conventional propeller), b) rake to suction side (also known as a tip fin or a Kappel propeller), c) rake to pressure side (also known as a tip rake propeller), (Dang, 2004)

An adaptation of the aerofoil winglet to ship propellers is to bend the blade tips, which was first introduced by Gomez et al(1998) by fitting an end plate towards the pressure side of a conventional propeller. This concept generated high efficiency for the propeller at heavy loading conditions compared to a conventional one; however, they ran a high risk of cavitation and efficiency loss at higher speeds. A similar adaptation was developed by Andersen et al(1986, 1997), where the propeller tip bends towards the blade suction side. The authors demonstrated that these forward-raked propellers had higher efficiency and good performance in open water and behind a ship. However, they showed higher pressure pulses compared to conventional design. A Japanese research group developed and designed aftward-rake propellers (Yamazaki et al 2005 and 2007). These propellers showed lower tip loading compared to forward-raked propellers. Okazaki et al(2015) revisited the concept and demonstrated that moderate aftward-raked propellers have little to no harmful effects on propulsive efficiency.

Brown et al(2014) examined the propulsive performance of tip-loaded propellers using potential flow simulations, Reynolds-Averaged Navier-Stokes (RANS) viscous flow simulations and experimental methods and offered insights into the Reynolds scaling methods for these propellers. The authors demonstrated the potential for improving efficiency and cavitation inception by implementing tip-loaded propellers, but the study was limited to open-water design and performance. Klose et al(2017) researched the tip-raked (aftward-raked) propellers and addressed the Reynolds number effect, intending to propose a Reynolds number correction/scaling procedure and ensure a fair comparison with different propeller designs. The authors also presented the influence of the scale on the cavitation behaviour in the simulated models and full-scale wake fields.

Gao et al(2019) utilized numerical techniques to investigate aftward-raked propellers by tilting the blade tip at six angles. The authors showed that the thrust coefficient gradually decreases with increased rake angle. The pressure coefficient (Cp) at the suction side of these propellers was higher than that of the conventional propeller in general. In addition, the tip tilts generated less cavitation behaviour when the rake angle was small. However, as the rake angle was further increased, the cavitation behaviour of the tip-raked propeller also increased, and it was even larger than that of the conventional propeller.

In more recent studies, Asif et al(2023), Chen et al(2023), and Du et al(2023) investigated different aspects of tip-raked propellers, primarily focusing on design optimizations and analysis. Chen et al(2023) applied a 4-order B-spline curve to design the rake distribution of Kappel (forward-raked propeller) propellers using five different tip rakes, and one type has no tip rake. The authors utilized a RANS method coupled with the g-transition model to analyze the open-water performance of the six propellers, considering cavitating flow. The research concluded that the tip rake is conducive to the thrust capacity of the Kappel propellers, mostly improving the propulsion efficiency by 2.5% at a designed advance speed with the appropriate tip rake. The author also found that an increase in the tip rake would magnify the low-pressure value and area on the suction side blade surface, together with the phenomenon of the stretching tip vortex and the inhibition of wake vortex contraction, which are both beneficial to the elevation of propulsion efficiency. However, the sheet cavitation behaviour aggravates as the tip rake rises. Overall, the forward-raked propeller favoured the propulsion performance, exhibiting the promising energy savings potential for the application to marine vehicles.

Asif et al(2023) investigated the open water, propulsion, cavitation and pressure pulse behaviour performance of forward- and aftward-raked propellers after establishing a decoupled design procedure by systematically controlling the blade geometry around the tip. Using a RANS-based approach and through experimental validations, the authors showed that even though cavitation increased for forward-raked propellers, the pressure pulse decreased compared to conventional and aftward-raked propellers. This study focused on the design procedure of tip-raked propellers and not the effect of rake distributions around the blade tips.

Du et al(2023) investigated conventional and winglet inboard (tip-raked) propellers in design optimization, analysis and testing under highly loaded conditions. The authors claimed that when appropriately designed, the tip-raked propellers can attain enhanced efficiency and reduced unsteadiness in propeller-induced forces acting on the hull's underside, compared to conventional propellers of the same overall diameter. Through full-scale testing of optimized conventional and tip-raked propellers installed on the same riverboat, the authors confirmed that the tip-rake design surpasses the optimal conventional propeller design, yielding a 13.2% improvement in fuel economy under light conditions and a 9.3% improvement under heavy conditions. These findings substantiate the advantages of utilizing winglet designs for propellers operating under highly loaded conditions.

The above studies indicate that both aftward- and forward-raked propellers could be designed to improve both propulsive and cavitation (hence pressure pulses and URN) performance. There appears to be a knowledge gap in understanding the effect of tip rake distributions on the hydrodynamic, cavitation and URN performance. The current paper focuses on the effect of the tip rake distributions on the open water and cavitation performance for both forward- and aftward-raked propellers. The effect of spanwise rake and skew distributions on the propulsive performance is also studied.

2 PROPELLER DESIGNS AND MODELLING

2.1 Propeller Designs

The tip-raked propeller designs were derived by following the conventional propeller design procedure and modifying the rake near the tip of an existing propeller designed for a container vessel. As such, this approach preserves the conventional cylindrical sections used to define the design propeller section; hence, it became a slightly rake-modified version of the existing design. The skew and tip-rake variants of the original (Base) propeller design were developed using a combination of in-house developed tools and commercially available CAD tools, SolidWorks and Hydrocomp's PropCAD software. A parametric model of the propeller is produced, where the propeller blade's geometric parameters and blade tip can be altered in various directions, ensuring that the profiles follow the cylindrical surfaces of a conventional design. The tip rake was simply varied by modifying the distribution of the normalized rake at the blade tip. This approach facilitates the rapid generation of tip rake variants by controlling the rake distributions, thus enabling the systematic study of propeller performance sensitivity to the selected rake distributions.

The study evaluated the original propeller (Base) with conventional cylindrical blade sections, one variation of the spanwise skew distribution of the Base (SK), three tip-raked aftward (towards pressure side) variants of Base (TA-1, TA-2 and TA-3), three tip-raked forward (towards suction side) variants of Base (TF-1, TF-2 and TF-3). The rake at the blade's tip is defined by the total rake at the tip and how sharply or softly this rake is achieved from zero rake at 0.7r of the blade (rake split radius). Figure 2 illustrates the rake distributions for both TF and TA propellers. The normalized rake values in the figure are the tangent values of the rake angles. For example, if the face of a propeller section is 0.2 m away downstream (aftward) from the directrix of the propeller and this section is located at a 2-m radial location, the rake value of this section is tan = 0.2/2=0.1. Note that for the geometry generation of the propeller blades, the skew distribution was applied first, which means the skew-induced rake was implemented before the rake distribution shown in Figure 2 was applied. Liu et al(2001) offer further details of the automated geometry generation technique utilized in the current research.

The main particulars of the Base propeller are shown in Table 1. Figure 3 shows the numerical model (top) and physical model testing (bottom) of the Base propeller, respectively. The parameters of the evaluated skew and rake variations are shown in Table 2.

Table 1 Base propeller particulars

Propeller Characteristics	Values
Number of Blades, Z	6
Diameter, D (mm)	250
Expanded Area Ratio, AE/Ao	0.789
Project Area Ration, AP/Ao	0.666
Pitch/Diameter, P/D at 0.7r	0.976
Skew (deg.)	29.5

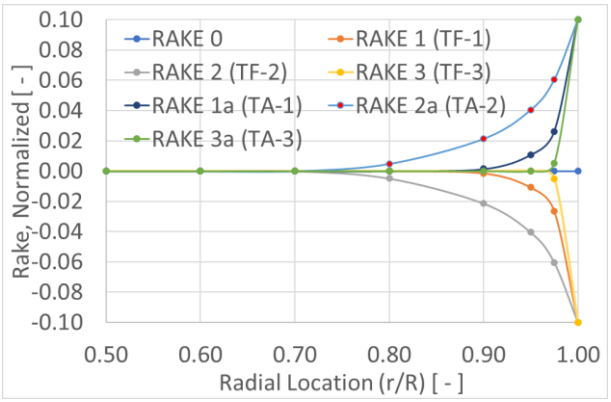

Figure 2 The definition of rake variants studied in this research.

All evaluated skewed and tip-raked propellers have diameters and blade geometry identical to the Base propeller with a split radius value of r/R=0.70. The nature of rake variations is defined as soft, moderate and hard, depending on how sharply or softly the maximum rake is obtained. Note that the Base propeller has both skew and rake distributions; however, for the investigation of the tip-raked propeller, the rake is modelled to be zero for all other propellers below r/R=0.70 of the blade. Figure 4 presents selected propeller geometry, capturing the variations of the rake,

skew and tip-rakes used for the PaTH-AC and RANS modelling and predictions.

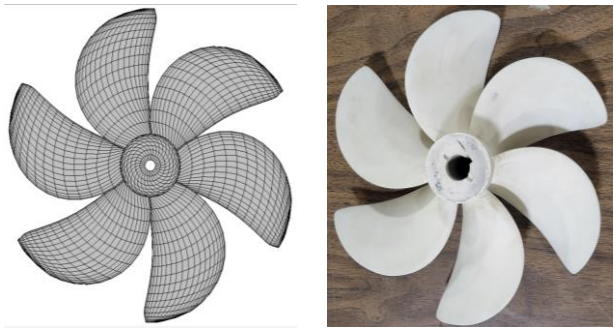

Figure 3 The Base propeller modelled for the PaTH-AC (left) and physical testing (right)

Table 2 The skew and rake parameters used in the current study

Test Cases	Rake Notation	Skew	Rake Variation	Normalized Rake at Tip
Base	Base	Base	Base	Base
Case0	No Rake	No Skew	NA	NA
Case1	No Rake	With Skew	NA	NA
Case2	TF-1	No Skew	Moderate	-0.1
Case3	TF-2	No Skew	Soft	-0.1
Case4	TF-3	No Skew	Hard	-0.1
Case2a	TA-1	No Skew	Moderate	0.1
Case3a	TA-2	No Skew	Soft	0.1
Case4a	TA-3	No Skew	Hard	0.1
Case7	TF-1	With Skew	Moderate	-0.1
Case8	TF-2	With Skew	Soft	-0.1
Case9	TF-3	With Skew	Hard	-0.1
Case7a	TA-1	With Skew	Moderate	0.1
Case8a	TA-2	With Skew	Soft	0.1
Case9a	TA-3	With Skew	Hard	0.1

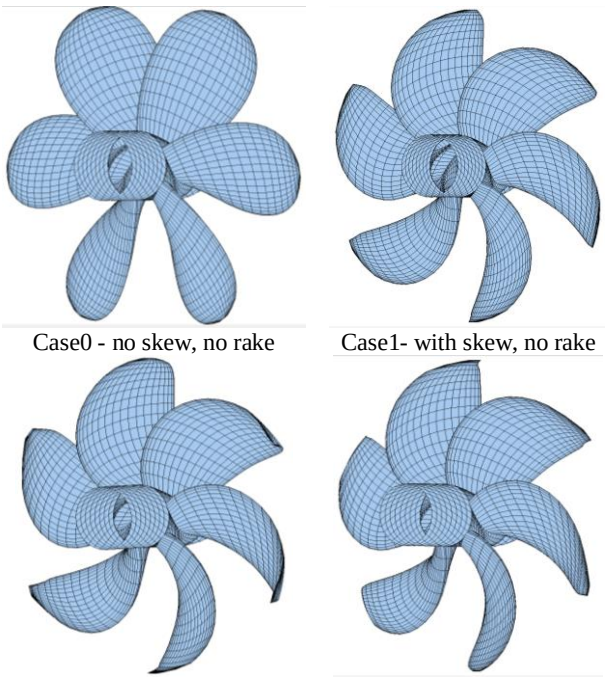

Figure 4 Example propeller geometry generated for the PaTH-AC modelling.

3 PHYSICAL AND NUMERICAL MODELLING

3.1 Physical Modelling

Physical model testing of the Base propeller was conducted in the towing tank facility at the Ocean Coastal and River Engineering Research Centre of the National Research Council Canada (the NRC-OCRE). This facility is 200m in length, 12m in width and 7m in depth. The model propellers were towed through still water by a carriage spanning the width of the tank. The carriage speed capabilities range from a minimum of 0.001 m/s to a maximum of 10 m/s. The instrumentation used for these experiments was the Kempf & Remmers dynamometer. This instrumentation package was selected based on its reputation for producing high-quality data. This particular dynamometer allowed for the measurement of propeller thrust and torque data over the selected range of advance coefficients required to characterize the performance of the propellers of interest. The NRC-OCRE standard testing procedure was followed to conduct the propeller open water tests (NRC 2004). The tests were completed for the advance coefficients ranging between 0 and 1.2 (or when the thrust becomes negative). More tests are planned for selected tip-raked propellers for both open water and cavitating conditions (with URN measurements) in the next testing phase.

3.2 PaTH-AC Modelling

The NRC-OCRE has been developing a panel method codebase for the modelling, predictions and post-processing for propeller and turbine hydrodynamics and acoustics (PaTH-AC) performance in cavitating and non-cavitating open water conditions. It is a low-order time-domain panel method formulated like many others (Katz & Plotkin 1991). The backbone of the current panel method code was initially developed to simulate marine swimmers with lunate tails (Liu 1996, Liu & Bose 1997, and Liu & Bose 1999). A refined and validated version of the code (formerly PROPELLA), was then developed for an ice-class propeller research program (Veitch et al 1997). Inflow wake and hyperboloid panel algorithms were also studied and implemented (Liu & Bose 1998), followed by a semi-empirical cavitation model to predict propeller cavitation performance (Liu et al 2001). This cavitation model has been utilized to predict the extent of cavitation for the Base propellers, the TF-1 and the TA-1 propellers. A more robust and reliable iterative pressure Kutta using Broyden's method, rather than the traditional Newton-Raphson method, was developed in 2002 (Liu et al 2002). Podded propeller geometry was implemented, and a comparative study between puller and pusher-type podded propulsors was performed (Islam 2004 and Islam et al 2006). A shed vortex impingement algorithm was developed recently (He et al 2007a and 2007b) and was validated via an in-house experimental research program (He et al 2005).

The code structure of PaTH-AC was changed to implement a multiple-body panel method formulation

for modelling propeller interacting with other objects, such as ice block, rudder, pod-structure, nozzle, etc. Detailed algorithm implementation of the multiple-object, multiple-path panel method to simulate the interaction between the propeller and other objects was given for an ice-class propeller approaching and interacting with an ice blockage (Liu et al 2008). This code was then validated and utilized to predict the performance of podded propulsors and the predicted forces and moments were also used as the basic data for estimating ship motion during maneuvering (Liu & Islam 2009).

The capability of the panel code has been further enhanced to model wind and tidal turbines by extending the modelling capability in the four quadrants of propeller operations (Liu 2010 and Liu et al 2018). In the latest endeavour, the PaTH-AC pre- and post-processing capabilities have been extensively enhanced to generate propellers and other geometries using raw propeller data as input and automated analysis and visualizations. The hydrodynamic kernel is being enhanced to incorporate a better fidelity cavitation model and to implement the Ffowcs Williams-Hawkings (FW-H) formulations for predicting the URN from propellers and other objects utilizing the surface pressure predicted by the panel code.

For the research, the simulation parameters used and the total number of simulations are summarized in Table 3. Note that the table provides all simulations completed in the research program, not necessarily presented in this paper. All simulations were conducted with the propeller shaft speed of 15 revolutions per second. According to the table, the total number of runs was 140 (so too is the number of input files). All the runs were made using a batch process. The runs were performed in an Intel(R) Xeon(R) Gold 5118 CPU @ 2.30GHz (2 processors, x64-based), w/512 cache with 128GB of RAM, Windows 10 Enterprise. On average, it took around two hours for each run. The simulation setup parameters used in the current study were selected using experience, and no panel size or time step sensitivity studies were conducted. The current paper presents results for open water simulations for all test cases. Two cases of cavitation simulations at a cavitation number of 2.75 are also presented in this paper.

Table 3 List of parameters used in the code for the predictions of propeller performance.

Parameters	Open Water	Cavitation
Spanwise Grid Type	Cosine	Cosine
Chordwise Grid Type	Cosine	Cosine
No. of Spanwise Intervals (Blades)	16	16
No. of Chordwise Intervals (Blades)	20	20
Front hub cone length	0.8D	0.8D
Rear hub cone length	0.8D	0.8D
No. of axial intervals (Front hub)	8	8
No. of axial Intervals (Rear hub)	8	8
No. of circular intervals (Front hub)	30	30
No. of circular intervals (Rear hub)	30	30
No. of intervals between blades	6	6
No of revolutions	3	3
Time steps per revolution	60	72
No of Propellers	11	3
The total number of Adv. Coefficients studied for each propeller	10	2
The total number of cavitation numbers studied for each propeller	NA	5

3.3 RANS Modelling

All RANS computations reported here are performed using the CFD software Star-CCM+. This commercial RANS solver is based on a finite volume (FV) method and starts from conservation equations in integral form. The governing (RANS) equations contain surface and volume integrals and time and space derivatives. These are then approximated for each Control Volume (CV) and time level using suitable approximations.

The RANS equations contain additional unknown variables, and a turbulence model is needed to determine those variables in terms of known quantities. The most prominent turbulence model for a RANS solver is the k-ω based Shear-Stress-Transport (SST) model developed by Menter (1994). This model was designed to give a highly accurate prediction of the onset and the amount of flow separation under adverse pressure gradients by including transport effects in the formulation of the eddy viscosity. All RANS simulations presented in this paper were completed using the k-ω SST turbulence model, considered the best compromise between numerical effort and computational accuracy.

The propeller's rotation in the fluid environment is generally modelled in a steady-state manner using the Moving Reference Frame (MRF) method or in an unsteady-state manner using the Sliding Mesh (SDM) method available in the RANS solver. The unsteady SDM is used to simulate the time-accurate behaviour of the propeller. The unsteady time-accurate solution is generally more applicable where flow swirl and extreme separation are expected to capture the non-uniform inflow to the propeller and the separation on unconventional blade geometry. In this approach, the mesh vertices of a propeller region move at the required rotational speed during a transient analysis. This mesh motion is specified using either a rotation or a rotation and translation motion. This technique was used for all simulations presented in this work. The unsteady sliding mesh approaches to propeller modelling require creating a separate region for the moving propeller blades and hub. The interface between the stationary and rotating regions is defined to provide special attention during the meshing process. Conformal meshes are preferred for the regions with the interface. A further discussion of these two approaches can be found in Islam (2015).

The propeller geometry (with and without the tip-rake geometry) was modelled in the RANS code by setting

up the geometry and generating the surface mesh, boundaries, volume mesh, solver, and physics. As described below, the setup was used for all RANS modelling conducted to maintain consistency in the comparative study. The fluid domain around the propeller is considered by a cylindrical frame within a rotating zone that envelops the propeller (excluding stationery bodies needed for future modelling). The simulation domain was a rectangular cube. The inlet and outlet positions are 5D and 10D from the propeller center, where D is the propeller diameter. The sides and bottom positions are 5D and 5D, respectively. Figure 5 shows the total 3D computational domain for the propeller in all configurations and operating conditions. Note that multiple blocks were used for the propeller and the wakes. These were set up as volumetric mesh refinement zones around the propeller to ensure the dominant flow characteristics were captured.

Unstructured polyhedral cells were used in the rotating block and static blocks. Using the unstructured grid results in a smoother discretization, particularly near the leading and trailing edge of the propeller. Figure 6 shows the volume mesh for a tip-rake propeller on a horizontal plane through the propeller center. To properly account for viscous effects and complex flow patterns, it is necessary to employ accurate and robust numerical methods to provide detailed resolution of the propeller boundary layer, turbulent wake, blade leading edge separation, and unsteady ring vortices induced by propeller operations. Extreme care was taken to arrange the meshing around the propeller blades. Figure 7 presents close-up views of the meshing arrangement around the Base propeller and tip-rake propeller blades. Local refinements were applied around the leading and trailing edges of the propeller blades. Additionally, 18 prism layers were applied to the propeller blades to ensure the high viscous effect was captured accurately near the boundary of the propeller blades.

One indication of how well the boundary layer on the propeller surfaces is discretized is the non-dimensional distance from a cell to the nearest wall, known as the Y+ value. Generally, if the wall Y+ value is sufficiently low (below 1), sufficient cells resolve the boundary layer flow down to the viscous sublayer. This method requires more cells and, therefore, more computational effort. Generally, a Y+ value between 0 and 5 is recommended to resolve the boundary layer flow, irrespective of the object's size. In the current simulations, the meshing arrangement is made such that a Y+ value between 0 and 5 is applied for both high and low Reynolds numbers treatment of the propeller blade surfaces. The values of the stretching factor, first cell height, total boundary-layer (prism layer) thickness and grid distribution have been set to have a range of Y+ of 0 to 5 in all current calculations and, at the same time, ensure a sufficiently smooth transition from the boundary layer mesh to the core flow mesh. The Y+ values on the Base and tip-rake propellers for a Reynolds number case under investigation are presented in Figure 8.

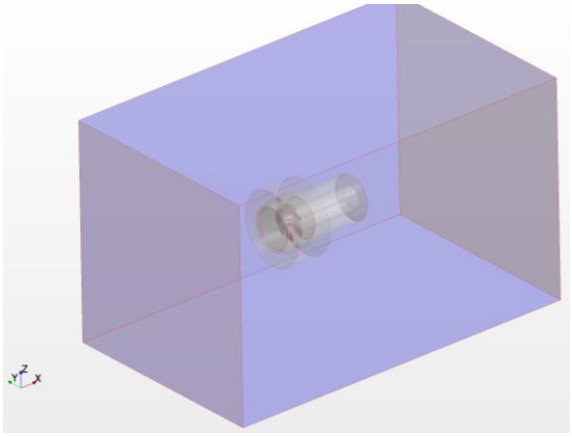

Figure 5 The mesh block model of the simulation field used for the RANS simulations of this study.

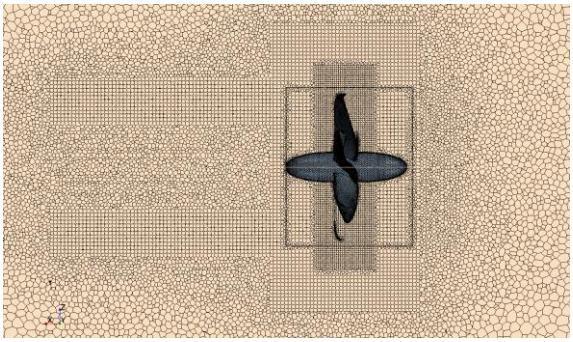

Figure 6 The horizontal plane showing the volume mesh around the Base propeller.

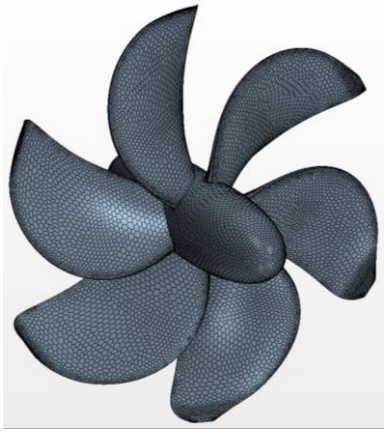

Figure 7 The close-up view shows the meshing arrangement around the tip-rake propeller.

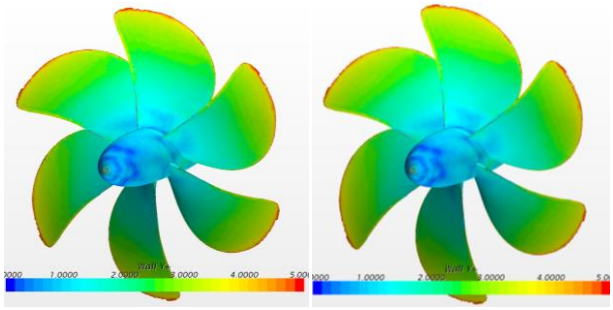

Figure 8 The Y+ values of the Base propeller for *J*=0.02 and right for *J*=0.08.

For the physics setup of the simulations, the inlet boundary condition was set as a velocity inlet with a constant velocity profile. The outlet boundary condition was set as a pressure outlet. The free surface was not modelled; a free slip wall was assumed instead. The propeller blades, hub and fairing cones and fixed cylinder were assumed to have no-slip wall boundary conditions.

The finite volume method solves the governing equations in the simulation. The SIMPLE algorithm is used to solve the pressure-velocity coupling equations. The second-order upwind discretization scheme is utilized for the momentum, turbulent kinetic energy, and turbulent dissipation rate. The propeller's rotation is modelled using the sliding mesh method, and turbulence is modelled by Menter's SST k-ω method (Menter 1994). The turbulence model is used in combination with all-y+ wall treatment.

The VOF (Volume of Fluid) method was adopted to model propeller cavitation and multiphase flow of water and vapour. Schnerr-Sauer cavitation model (Schnerr & Sauer 2001) based on the reduced Rayleigh-Plesset equation (Plesset 1977) was implemented in the RANS model. Although the cavitation is influenced by many parameters such as velocity, density, viscosity, saturation and static pressures, surface tension and so on, this method, in contrast to the full Rayleigh-Plesset model, neglects the influence of bubble growth acceleration, surface tension as well as viscous effects between water and vapour phases (Star CCM+ User Guide 2018). For the cavitation simulations, the slightly refined meshing arrangement was used to estimate the hydrodynamic performances of the propellers in cavitating conditions using Star CCM+. A new refined grid was generated for each propeller to capture the bubbles.

The simulation conditions planned in this work are presented in Table 4. The simulation time is approximate and based on the CPU time required in an Intel(R) Xeon(R) CPU E5-1650 v2@3.50GHz machine with 16 GB memory. The cavitation simulation results presented here were carried out for the Base and Case7 (TF-1) propellers, each at propeller loading condition of J=0.8 and at a cavitation number, σ_n =2.75. This paper presents the results completed to date. All simulations were conducted with the propeller shaft speed of 15 revolutions per second.

Table 4 RANS simulation conditions examined in the study.

Case	Simulation Type	Adv. Coeff.	Cav #	Total Mesh(M)	Time (hrs)
1	Open Water	0.2, 0.5, 0.8, 1.0	NA	2.25	20h
1	Cavitation	0.2, 0.8	2,2.75,3.5	2.75	60h
7	Open Water	0.2, 0.5, 0.8, 1.0	NA	2.25	20h
7	Cavitation	0.2, 0.8	2,2.75,3.5	2.75	60h
7a	Open Water	0.2, 0.5, 0.8, 1.0	NA	2.25	20h
7a	Cavitation	0.2, 0.8	2,2.75,3.5	2.75	60h

The meshing arrangement and other simulation parameters were selected for all RANS simulations using previous experience (Islam et al 2015). All simulations were targeted to run sufficiently long to obtain convergence (insignificant variations of thrust/torque over time), typically up to 1.0 seconds for unsteady state simulations for the cavitation cases. A time step equivalent to 6° and 2° rotation of the propeller shaft per time-step was used for the open water and cavitation simulations, respectively. The number of inner iterations per time step for both cases was 15.

4 RESULTS AND DISCUSSIONS

For both PaTH-AC and RANS simulations, the propeller thrust and torque were predicted at the propeller hub center and presented in traditional non-dimensional coefficients as defined in Table 5. The list shows that for the cavitation simulations, the nominal cavitation numbers were based on propeller revolutions instead of propeller advance speed or propeller resultant speed. This formulation presented the performance in terms of thrust coefficient, K_T or torque coefficient, K_Q against cavitation number, which was not a function of advance coefficient, J.

Table 5 Data reduction equations and definitions of parameters used to present the experimental data.

Performance Characteristics	Data Reduction Equation
K_T - propeller thrust coefficient	$T / \rho n^2 D^4$
$10K_Q$ - propeller torque coefficient	$10Q / \rho n^2 D^5$
J - propeller advance coefficient	V_A / nD
η_{Prop} - propeller efficiency	$J / 2\pi \times (K_T / K_Q)$
σ_n - Cavitation number	$\sigma_n = \frac{P_{amb} + \rho g h - P_V}{\frac{1}{2}\rho n^2 D^2}$
where, T - propeller thrust; Q - propeller torque; ρ - water density; n - propeller rotational speed; D - propeller diameter; V_A - propeller advance speed, in the direction of carriage motion; P_{amb} - atmospheric pressure, P_V - saturation pressure of water at the test condition; h - static height of shaft centre relative to the free surface.	

4.1 Models Validations

As the first step in the model validation, the comparison between measurements, RANS and PaTH-AC predictions of the propulsive performance of a base propeller in a range of loading conditions is carried out. The measurements and predictions of the open water characteristics of the Base propeller are presented in Figure 9, which shows a good agreement. The RANS predicted time-averaged thrust and torque were within 2% and 4% of the measurements, respectively, based on the comparisons of three data points. The RANS simulations were still being carried out while this paper was being written. The PaTH-AC predicted thrust and torque were within 10% and 4% of the measurements, respectively, based on the comparisons of the entire range of loading conditions. The overpredictions by

PaTH-AC were large at high loading and tapered down fast with decreasing loading condition. This indicated that the PaTH-AC provided better predictions at moderate loading than high loading condition.

The comparison of RANS and PaTH-AC propulsive performance of the Base and TF-1 (Case7) propellers for different propeller loading conditions is provided in Figure 10. It is noted that both the thrust and torque of the TF-1 propeller are higher than that of the Base propeller, which both RANS and PaTH-AC models predicted. This confirms that the PaTH-AC model can capture the effect of the tip rake on the propulsive performance, similar to the RANS model. The physical testing of the TF-1 propeller will be completed during summer of 2024.

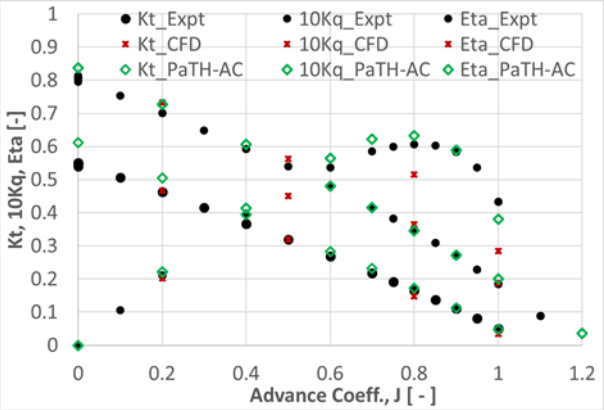

Figure 9 Open water characteristics of the Base propeller comparing the RANS and PaTH-AC predictions with the corresponding measurements.

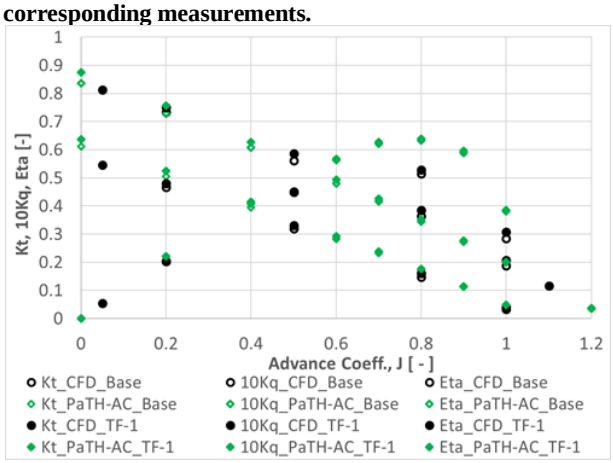

Figure 10 Open water characteristics of the Base and the tip-raked propeller comparing the RANS and PaTH-AC predictions.

Figure 11 and Figure 12 show the RANS predicted blade surface pressure on the pressure and suction sides of the Base and TF-1 propeller at J=0.02 and J=0.8, respectively. The change in the pressure distributions around the tip of the forward-raked propeller is evident for both loading conditions, particularly on the suction sides. The lower pressure peak covering a larger area at the suction side around the tip explains the higher thrust and torque of the TF-1 propeller compared to the Base propeller at both loading conditions.

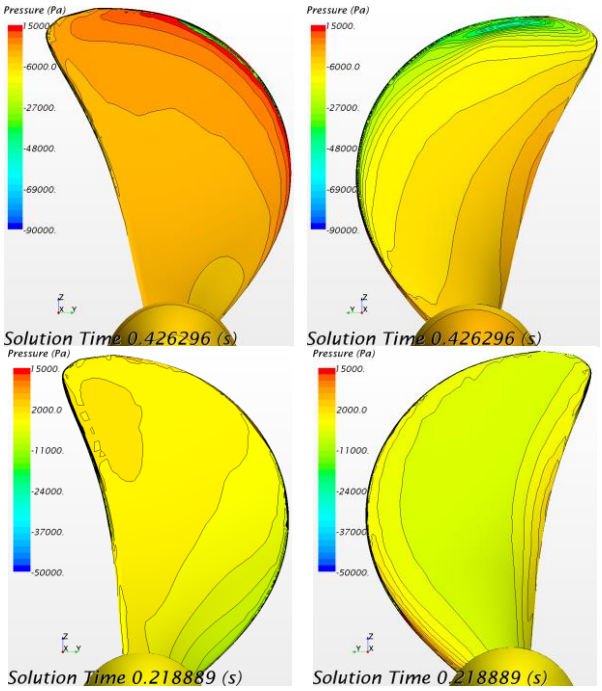

Figure 11 The RANS predicted surface pressure of the Base propeller blade: Top - at J=0.2, on the pressure side (left) and suction side (right); Bottom - at J=0.8, on the pressure side (left) and suction side (right);

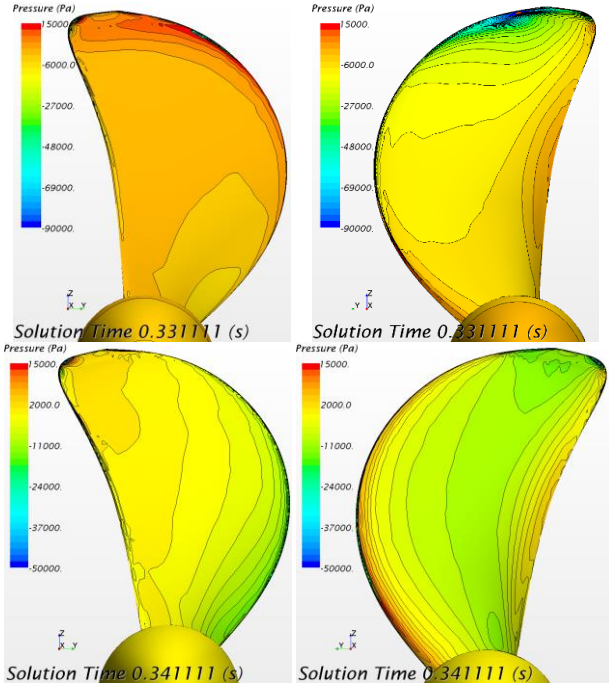

Figure 12 The RANS predicted surface pressure of Case 7 (TF-1) propeller blade: Top - at J=0.2, on the pressure side (left) and suction side (right); Bottom - at J=0.8, on the pressure side (left) and suction side (right);

4.2 Effect of Rake and Skew

Comparisons of the Base propeller's performance with and without the spanwise distributions of skew and rake of the blades are carried out using PaTH-AC. Figure 13 shows that the presence of a moderate amount of rake (~5° at the tip) in the blade does not significantly (< 1%) change the thrust and torque at any loading condition. Figure 14 shows that a moderate amount of blade skew (~25° at the tip) significantly lowered both thrust and

torque, particularly at high-loading conditions. This combined outcome encourages the study of the effect of tip-rake for both skewed and non-skewed propellers.

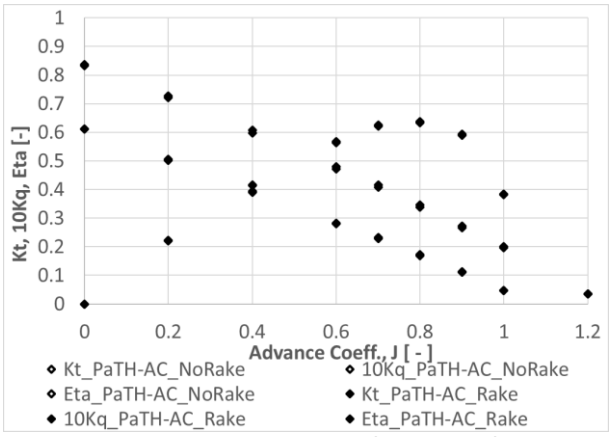

Figure 13 PaTH-AC predicted performance of propellers with and without blade rake.

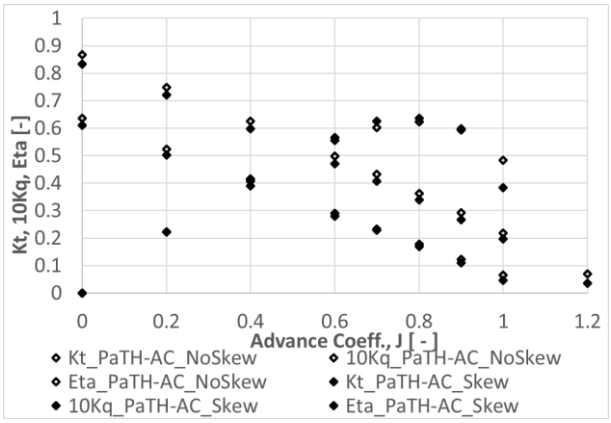

Figure 14 PaTH-AC predicted performance of propellers with and without blade skews.

4.3 Tip-Raked Propellers

A comparative study for the forward- and aftward-raked propellers based on PaTH-AC predictions is carried out in this section; see Figure 15 through Figure 20. The following remarks are made based on each propeller's open water characteristics (K_T, K_Q, and efficiency) over the range of loading conditions, with advance coefficients of J=0.0 to J=1.2.

The thrust and torque of a forward-raked propeller (both skewed and non-skewed blades) is generally higher than that of a propeller without the tip rake in all loading conditions, see Figure 15 and Figure 17. The predicted efficiencies of the two forward-raked propellers are also higher than those propellers without tip-raked.

The thrust, torque, and efficiency of an aftward-raked propeller (both skewed and non-skewed blades) is lower than that of a propeller without the tip rake in all loading conditions, see Figure 16 and Figure 18.

For a constant tip rake value, the rate of increase of the tip rake generally influences the change in the thrust and torque, irrespective of the direction of the rake. Generally, the soft change in the rake has a larger influence on the change in the thrust and torque than the moderate change in the rake; the hard change in the rake has the least influence on the change in the thrust and torque in open water conditions.

Figure 19 and Figure 20 present the thrust of the forward- and afterward-raked propellers relative to the Base propeller for the non-skewed and skewed propellers, respectively. Overall, a forward-raked blade tip results in a larger propeller thrust and torque than the aftward-raked ones when the rate of change of the rake remains the same. This is true for all loading conditions. This effect is more pronounced when the blades are skewed compared to the corresponding non-skewed propellers. This tells that the influence of the tip-rake is more significant for the skewed propellers. Further studies using RANS and physical tests to evaluate and confirm the effects of tip rake are recommended for highly skewed and highly raked propellers.

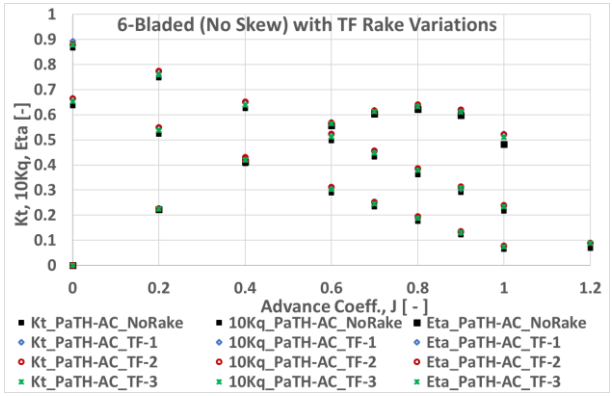

Figure 15 PaTH-AC predicted performance of non-skewed forward-raked propeller with tip rake variants.

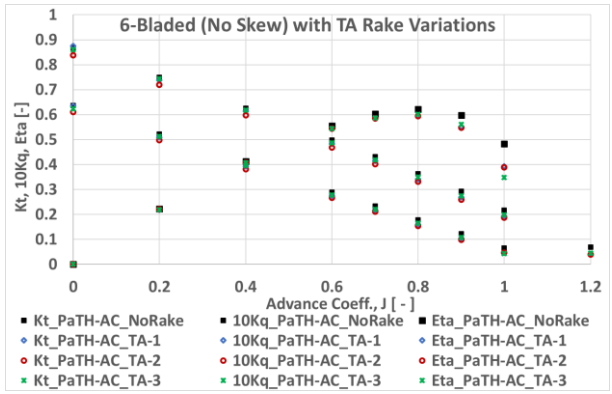

Figure 16 PaTH-AC predicted performance of non-skewed aftward-raked propeller with tip rake variants.

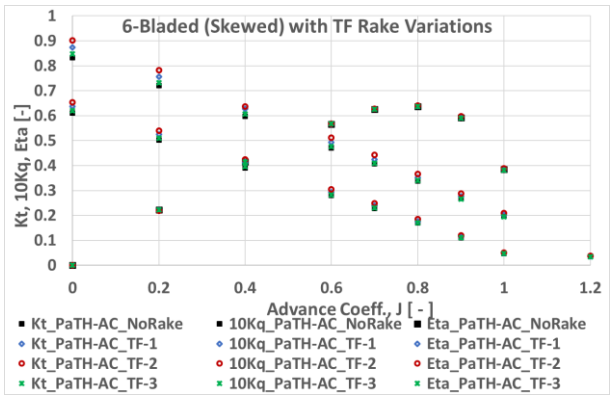

Figure 17 PaTH-AC predicted performance of skewed forward-raked propeller with tip rake variants.

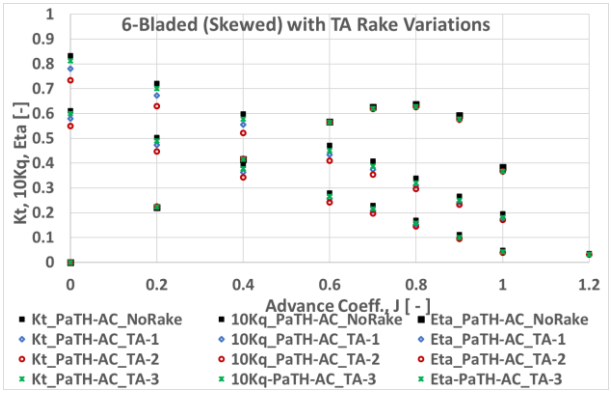

Figure 18 PaTH-AC predicted open water performance of skewed aftward-raked propeller with tip rake variants.

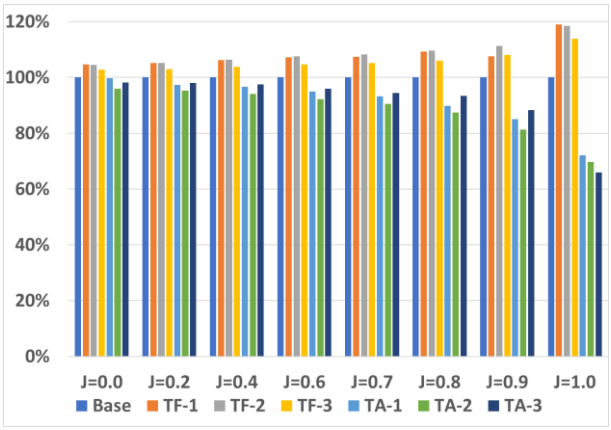

Figure 19 The thrust of the tip-raked non-skewed propellers compared with the Base propeller.

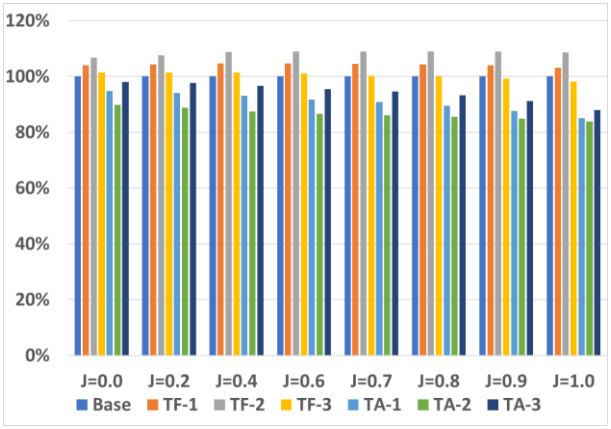

Figure 20 The thrust of the tip-raked skewed propellers compared with the Base propeller.

Note that the panel distribution used in the PaTH-AC simulations for the propeller with a hard rake (see Figure 4) does not decrease monotonically (cosine) as in the other propellers. This may have resulted in insufficient pressure data to obtain smooth interpolation at the tip. Improving the panel distribution around the tip with a hard rake may offer a more accurate prediction of pressure distribution.

4.4 Tip-Raked Propeller Cavitation

Limited cases of the Base propeller and Case 7 (TF-1) propellers were studied for the cavitation case at σ_n=2.75. The preliminary RANS predicted sheet cavitation for these two propellers are presented in Figure 21 and Figure 22. These preliminary results show higher amounts of sheet cavitation around the blade lower end and the tip for the TF-1 propeller and traces (insignificant) of cavitation in similar blade areas for the Base propeller. The preliminary PaTH-AC model also showedsheet cavitation in similar areas for the TF-1 propeller, see Figure 23.

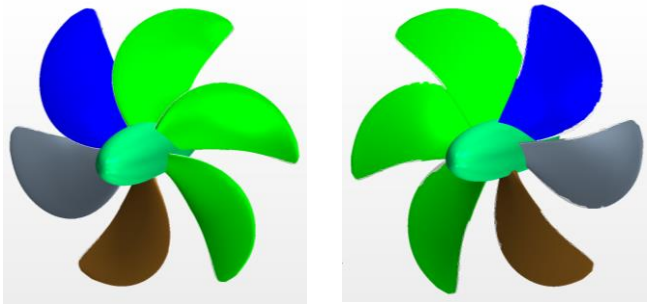

Figure 21 The RANS predicted sheet cavitation on the Base Propeller at *J*=0.80 and σn=2.75; left-suction side and right-pressure side.

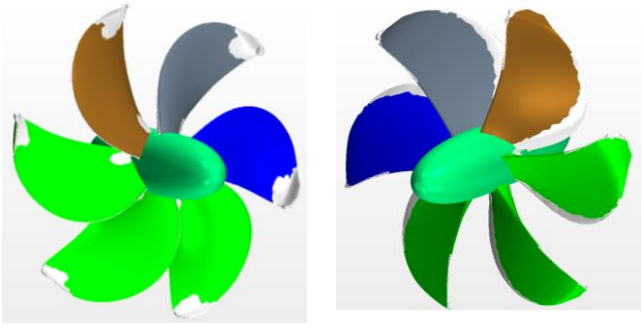

Figure 22 The RANS predicted sheet cavitation on the tip-rake (TF-1) Propeller at *J*=0.80 and σn=2.75; left-suction side and right-pressure side.

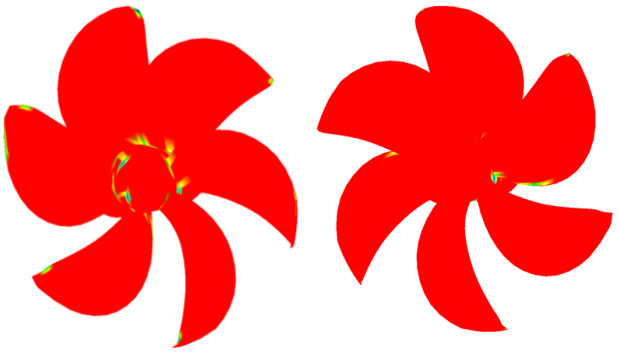

Figure 23 The PaTH-AC predicted sheet cavitation on the tip-rake (TF-1) Propeller at *J*=0.80 and σn=2.75; left-suction side and right-pressure side.

The cavitation predictions are considered preliminary as both PaTH-AC and RANS simulations for the propellers under cavitation conditions were conducted using coarse panel/mesh, and local blade and wake refinements were not done to capture the probable sheet and tip vortex cavitation an in-house developed panel method code.

5 CONCLUDING REMARKS

This paper presents the preliminary outcome of a research program for investigating the effect of orientations and configurations of tip-raked propellers, which includes predictions of propeller thrust and torques as well as cavitation characteristics at different propeller loading conditions. A Reynolds-Averaged

Navier Stokes (RANS) solver and an in-house developed panel method code (PaTH-AC) are used to predict the propulsive performance of the tip-raked propellers.

Good agreements between the PaTH-AC and RANS predictions and measurements for a Base propeller thrust and torque were achieved for different loading conditions. Both models captured well the trends of tip-rake dependency for both thrust and torque under different loading conditions. A review of the pressure distribution on the tip-raked blade and the velocity distribution around the propulsor demonstrated the complex interactions between the propeller tip flow, wake and inflow. It revealed the significant effect of the propeller tip geometry on the 3D flow around the propulsor.

A comparative study of propellers with and without rake and skew and with forward- and aftward-raked blades was carried out, and the following remarks are made based on the findings.

- A moderate change in the spanwise rake of the blades does not significantly change the thrust and torque of a propeller.
- A moderate change in the spanwise skew of the blades can significantly lower the thrust and torque of a propeller.
- The thrust and torque of a forward-raked propeller are generally larger than that of a propeller without the tip rake in all loading conditions.
- The thrust and torque of an aftward-raked propeller are generally smaller than that of a propeller without the tip rake in all loading conditions.
- The rate of increase of the tip rake generally influences the change in the thrust and torque, irrespective of the direction of the rake.
- A forward-raked blade tip results in a higher thrust and torque than the aftward-raked blade when the rate of change of the rake remains the same. This effect is more pronounced when the blades are skewed as compared to the corresponding non-skewed propellers.

This study demonstrates that the PaTH-AC codebase, with proper panel arrangement, boundary conditions and setup techniques, can predict the performance characteristics of the tip-raked propulsor in various loaded conditions with the same level of accuracy as the industry standard RANS solver and physical measurements. The author believes this research program will enhance numerical simulation capability to capture most hydrodynamics of any novel propulsion system, such as highly skewed tip-raked propulsors.

The results presented in this paper are limited to open-water design and the performance of propellers with the same geometric parameters except for changes in the rakes at the blade tip. The authors plan to continue this research by optimizing both the PaTH-AC and RANS model setup for more accurate propulsive performance and cavitation predictions. Also, it is recommended to continue this research for the predictions of the performance of tip-raked propellers in the ship wake (i.e. non-uniform inflow including radial and tangential components) to assess the effects of more realistic flow fields on the efficiency, cavitation and URN performance.

ACKNOWLEDGEMENTS

The authors thank National Research Council of Canada for the financial support of this research program.

REFERENCES

Asif, A., Kleinsorge, L., Greitsch, L. (2023). 'A Contribution to the Design and Numerical Evaluation of Unconventional Tip-Rake Propeller', Proceedings of the Thirty-third (2023) International Ocean and Polar Engineering Conference www.isope.org, Ottawa, Canada, June 19-23.

Anderson. P. (1997). 'A comparative Study of Conventional and Tip-Fin Propeller Performance', Twenty-First Symposium on Naval Hydrodynamics, 934.

Andersen, S. V. & Andersen, P. (1986). 'Hydrodynamic Design of Propellers with Unconventional Geometry', Transactions of The Royal Institution of Naval Architects, 201-221.

Brown, M., Sánchez-Caja, A., Adalid, J.G., Black, S., Sobrino, M.P., Duerr, P., Schroeder, S., Saisto, I. (2014). 'Improving propeller efficiency through tip loading', 30th Symposium on Naval Hydrodynamics Hobart. University of Tasmania-UTAS.

Chen, C.-W., Chen, X.-P., Zhou, Z.-Y., Chen, L.-W., Zhang, C., Zheng, T.-J., Li, H.-M. (2023). 'Effect of Tip Rake Distribution on the Hydrodynamic Performance of Non-Planar Kappel Propeller', Journal of Marine Science and Engineering, 11, 748. https://doi.org/10.3390/jmse11040748.

Dang, J. (2004). 'Improving Cavitation Performance with new Blade Sections for Marine Propellers', 9th Inter-national Symposium on Practical Design of Ships and other Floating Structures, Lübeck-Travemünde.

Du, W., Gunderson, A., Reifsnyder, J., Farrell, K. (2023). 'Design, analysis and test of conventional and winglet propellers under highly loaded conditions', Ocean Engineering 284, 115173, https://doi.org/10.1016/j.oceaneng.2023.115173

Gao, H., Zhu, W., Liu, Y., Yan, Y. (2019). 'Effect of various winglets on the performance of marine propeller', Applied Ocean Research, 86, 246–256.

Gomez, P. & Gonzalez-Adalid, J. (1998). 'Detailed Design of Ship Propellers', FEIN, Madrid.

Klose, R., Schulze1, R., Hellwig-Rieck, K. (2017). 'Investigation of Prediction Methods for Tip Rake Propellers', Fifth International Symposium on Marine Propulsors SMP'17, Espoo, Finland, June.

He, M., Veitch, B., Bose, N., Bruce, C. and Liu, P. (2005). 'Numerical Simulations of Propeller Wake Impacting on a Strut', Proceedings of the CFD2005, St John's, NL Canada, August, 8p.

Islam, M. Veitch, B., Bose, N. and Liu, P. (2006). 'Numerical Study of Hub Taper Angle on Podded Propeller Performance', Journal of Marine Technology, Vo. 43, No.1, pp.1-10.

Islam, M. F., Taylor, R., Quinton, J., Veitch, B., Bose, N., Colbourne, B. and Liu, P. (2004). 'Numerical investigation of propulsive characteristics of podded propeller', Proceedings of the 1st International Conference on Technological Advances in Podded Propulsion, Newcastle University, UK, April, pp. 513-525.

Islam, M. F., Jahra, F., Ryan, R., Hedd, L. (2015). 'Hydrodynamics of podded propulsors with highly loaded propellers and in extreme azimuthing conditions', Proceedings of the 33rd International Conference on Ocean, Offshore and Arctic Engineering, OMAE 2015, May 31 - June 5, 2015, St. John's, NL Canada.

Katz, J. & Plotkin, A. 91991). 'Low-speed Aerodynamic d from Wing Theory to Panel Methods', McGraw-Hill, Inc., New York, 1991.

Liu, P. (1996). 'A Time-domain Panel Method for Oscillating Propulsors with Both Spanwise and Chordwise Flexibility', Ph.D. thesis, Memorial University of Newfoundland.

Liu, P., Bose, N., Colbourne, B. (2001). 'Incorporation of a critical pressure scheme into a time-domain panel method for propeller sheet cavitation', International Workshop on Ship Hydrodynamics, Wuhan, China, 2001, p. 9

Liu P. & Bose N. (1998). 'An unsteady panel method for highly skewed propellers in nonuniform inflow', 22nd ITTC propulsion committee propeller RANS/Panel method workshop, 5-6 April, Grenoble, France, p. 343e49.

Liu P, Bose N, Colbourne B. (2001). 'Automated marine propeller geometry generation of arbitrary configurations and a wake model for far-field momentum prediction', International Shipbuilding Progress,48(4):351e81.

Liu P, Bose N, Colbourne B. (2002). 'A broyden numerical Kutta condition for an unsteady panel method', International Shipbuilding Progress, 49 (4):263e73.

Liu P, Akinturk A, He M, Islam M, Veitch B. (2008). 'Hydrodynamic performance evaluation of an ice class podded propeller under ice interaction', OMAE2008- 57013. Proceedings of 27th International Conference on Offshore Mechanics and Arctic Engineering, 9 p.

Liu, P., Islam, M., Veitch, B. (2009). 'Some Unsteady Propulsive Characteristics of a Podded Propeller Unit under Maneuvering Operation', First International Symposium on Marine Propulsors Smp'09, Trondheim, Norway, June.

Liu, P. (2010). 'A computational hydrodynamics method for horizontal axis turbine-panel method modelling migration from propeller to the turbine', Energy 35 (2010) 2843e2851.

Liu, P., Bose, N., Chen, K., Xu, Y. (2018). 'Development and optimization of dual-mode propellers for renewable energy', Renewable Energy, Volume 119, 2018, Pages 566-576, ISSN 0960-1481, https://doi.org/10.1016/j.renene.2017.12.041.

Murdy, D. (2004). 'Propeller Open Water Tests', IOT Standard Test Method TM-2, V6.0, April.

Okazaki A, et al (2015). 'The Effect of Tip Rake on Propeller Open Water Efficiency and Propulsive Efficiency', Fourth International Symposium on Marine Propulsors, 4-7.

Prandtl, L. & Betz, A. (1927). 'Der induzierte Widerstand von Flügeln mitEndscheiben', Ergebnisse der Aerodynamischen Versuchsanstalt zuGöttingen, III. Lieferung. Verlag R. Oldenburg, München und Berlin.

Plesset, M. S. & Prosperetti, A. (1977). 'Bubble Dynamics and Cavitation'. The Annual Review of Fluid Mechanics, Vol 9.

Schnerr, G. H. & Sauer, J. (2001). 'Physical and Numerical Modelling of Unsteady Cavitation Dynamics'. International Conference on Multiphase Flow, New Orleans, USA.

Yamasaki, S. & Okazaki, A. (2005). 'Cavitation Test on a Straight Leading Edge Propeller and a Tip Rake Propeller', Journal of the Japan Society of Naval Architects and Ocean Engineers, Vol. 2, 271-277

Yamasaki, S. & Okazaki, A. (2007). 'Design and model tests of a backward tip rake propeller for a low speed ship', Journal of the Japan Society of Naval Architects and Ocean Engineers, Vol. 5, 163-168.